JOURNAL OF CATALYSIS 45, 198–215 (1976)

Structural Changes in Thin Films of the 1:1 Bismuth Molybdate under Reduction and Oxidation Conditions

JITENDRA KUMAR AND ELI RUCKENSTEIN[1]

Faculty of Engineering and Applied Sciences, State University of New York at Buffalo, Buffalo, New York 14214

Received March 8, 1976; revised August 30, 1976

A systematic study of reduction and reoxidation of thin films of 1:1 bismuth molybdate was carried out using transmission electron microscopy and electron diffraction. Films 50–700 Å thick prepared by the vacuum evaporation technique have been subjected to further oxygen depletion (reduction) by annealing in vacuum and to reoxidation by heating in air. The films obtained by vacuum evaporation were found to be amorphous and oxygen deficient. On oxidation, pronounced recrystallization occurred and a scheelite tetragonal phase was found with parameters $a = b = 5.26 \pm 0.05$ Å, $c = 11.52 \pm 0.05$ Å, $c/a \sim 2.19$ and space group $I4_1/a$ (C_{4h}^6). Further heating in air resulted in the nucleation and growth of smaller crystallites (domains) of a different structure (superstructure) within the previously developed single crystals. The new structure corresponds to a body centered tetragonal cell having the parameters $a = b = 5.32 \pm 0.05$ Å, $c = 11.70 \pm 0.05$ Å, $c/a \simeq 2.2$ and space group $I\bar{4}m2$ (D_{2d}^9). By heating the original films in vacuum, however, further oxygen depletion occurred along with the usual crystallization, yielding finally MoO_2, metallic bismuth and traces of the scheelite structure. The structure of the region near the catalyst surface differs from the structure of the bulk. Thin films may possibly provide some information about the structure of this region. Furthermore, catalytic oxidation by oxides is essentially a reduction of the catalyst followed by its reoxidation by the oxygen of the atmosphere. Therefore, we suggest that a switching between a scheelite structure during the reduction period and the superstructure during the catalyst reoxidation period may occur in the region near the surface of the catalyst. Some considerations are provided regarding the hypothesis that some nonstoichiometric compounds contain within the initial compound a dispersion of small particles with a different composition.

INTRODUCTION

The bismuth molybdates have numerous applications as catalysts in oxidation reactions of industrial importance (*1*, *2*). This, in turn, has led to many investigations concerning their physicochemical properties, catalytic activity, selectivity, and reaction mechanisms. These studies have shown that only the compounds having Bi/Mo atomic ratios between 2:3 and 2:1 are useful as catalysts. At least three distinct molybdates are found in this range, viz,

$Bi_2Mo_3O_{12}$	(2:3)	α-phase
$Bi_2Mo_2O_9$	(1:1)	β-phase
Bi_2MoO_6	(2:1)	γ-phase

which occur in different crystallographic modifications (*3*). According to Batist *et al.* (*4*), both the 1:1 and 2:1 molybdates are highly active and selective, whereas the 2:3 is selective but weakly active for oxidation of olefins. The existence of an amorphous phase in the bismuth molybdate system was also reported and thought to be

[1] Correspondence concerning this paper should be addressed to E. Ruckenstein.

even more active than the crystalline phases (*5*).

Although the structural crystallography of the 2:3 and 2:1 compounds have been worked out in detail (*6*, *7*), this is not true for the comparatively less studied 1:1 molybdate. In 1964, Erman *et al.* (*8*) proposed a unit cell for $Bi_2Mo_2O_9$ with parameters $a = b = 11.8$ Å and $c = 5.4$ Å. In a subsequent note, however, Erman and Galperin (*9*) reported more precise parameters as $a = 10.79$ Å, $b = 11.89$ Å, and $c = 11.86$ Å; hence, apart from a slightly orthorombic distortion a unit cell with one of its dimensions doubled. Batist *et al.* (*4*) obtained X-ray diffraction data for the 1:1 compound related but not identical to those of Erman *et al.* (*8*, *9*) and were inclined to assume a long *c*-axis of 54 Å. Based on infrared studies they assumed the molybdenum ions in octahedral configurations with corner sharing of octahedra. On this basis they built up the structure of 1:1 molybdate by connecting the end of the $(Bi_2O_2)^{2+}$ layers with double layers of Mo–O octahedra having the ReO_3 structure. However, spectroscopic studies (*10*) revealed the presence of both the tetrahedral and octahedral oxomolybdenum species on active molybdate catalyst surfaces. Schuit (*1*) concluded in a recent review that the structure of the 1:1 molybdate is unclear and that the compound itself is thermally unstable. The structural information available so far refers to the bulk of the catalysts, while the catalytic properties are determined by the region near the surface which can have a different structure. Thin films may, however, give some information about the structure of this region. Further, the mechanism of oxidation of olefins involves the oxygen of the catalyst itself. The role of gaseous oxygen is simply to replenish the oxygen of the lattice of the catalyst. Indeed, oxidation of olefins is known to occur in the absence of oxygen also (*11*). This means that the process is essentially a reduction of the catalyst followed by its reoxidation by the oxygen of the gaseous atmosphere. As a result, significant changes in structure and activity of the catalyst can take place during the catalytic oxidation. The present investigation was, therefore, carried out to obtain information concerning the structural modifications of thin films of 1:1 bismuth molybdate during reduction and subsequent reoxidation processes. The reduced catalyst was obtained by forming thin films in a high vacuum coating unit and the regeneration was carried out by heating the thin films in air. The thin films were examined in a transmission electron microscope, which has the advantage of providing information on both the microstructure and the structural crystallography. Like for the thin films of other compounds (*12*), one may expect that in some conditions thin films of bismuth molybdate exhibit phases normally unstable or not found in bulk materials. They might, however, occur in the layer near the surface of a catalyst during the catalytic process. After prolonged heating of sufficiently thick films, the phases are probably those of the bulk material.

EXPERIMENTAL METHODS

a. Preparation of the 1:1 Compound

Ammonium molybdate obtained from Ventron Corp. was heated in air at 700°C for about 48 hr to yield pure MoO_3. Bismuth oxide was prepared by dehydrating bismuth nitrate supplied by Fisher Scientific Co. and then calcining in air at 600°C for 24 hr. Thereafter, both oxides were crushed to powder separately and mixed in proportions such that the atomic ratio Bi/Mo was unity. A pellet was then made from the well-mixed powder at 10 atm pressure and heated in air at 765°C for 24 hr. After cooling, the pellet was crushed to powder and annealed in air at 600°C for 24 hr. The resulting product was the working material. Bismuth molybdate of the

same composition was also procured from Climax Molybdenum Co. and from the laboratory of Dr. Ph. A. Batist. X-Ray diffraction was used for the identification of various phases present in the samples.

b. Thin Film Preparation

Resistive heating of powder samples to vaporization was carried out under vacuum ($\sim 10^{-6}$ Torr) in a precleaned molybdenum boat. The molybdate vapor so formed was deposited onto single crystals of air cleaved rock salt held just above the boat. The thickness of the films varied from 50 to 700 Å and were computed from the values of the total mass evaporated, the density of bulk molybdate and the distance of rock salt to the boat. The 50 Å film consisted of discontinuous islands and was not a film in the strictest sense of the word: the value supplied is an effective, or "smoothed" thickness. Portions of these films were calcined in air for 30 min at temperatures ranging from 25 to 500°C and at 250°C for up to 72 hr. In addition, vacuum annealing of films was carried out in a few cases at 230°C for 1 hr. The rock salt crystal was chosen as substrate because the samples could be conveniently handled and heat treated. Also, it allowed the transfer of thin films without damage and with ease to a water surface from where they could be picked up on copper grids for subsequent electron microscopy and electron diffraction experiments. Electron micrographs and corresponding diffraction patterns were recorded from different regions and analyzed. For computing the interplanar spacings (d-values) corresponding to various diffraction rings and/or spots, the camera length was determined in the usual way using the films of gold as standard (*13*).

RESULTS AND DISCUSSION

a. X-Ray Work

X-Ray patterns of bismuth molybdate powders were obtained using a nickel filtered CuK_α radiation in a Norelco Diffractometer. The interplanar spacings (d-values) were determined precisely from the diagrams and relative intensities of lines were noted from the diffraction peak heights. The various phases present in the samples were identified by comparing the computed d-values with the characteristic lines of different compounds of the bismuth molybdate system (*8*, *14*). The samples procured from Climax Molybdenum Co. show the simultaneous presence of 1:1 and 2:3 compounds and, in addition, Bi_2O_3. This material was therefore melted and kept near 800°C for about 15 min, cooled slowly to 600°C and calcined at this temperature for 24 hr. By cooling to room temperature slowly, X-ray examination showed the presence of mainly the 1:1 compound with traces of the 2:3 compound as in the bismuth molybdate prepared by us. The d-values and corresponding relative intensities are given in Table 1. These

TABLE 1

d-Values and Corresponding Relative Intensities as Observed in X-ray Diagrams for the 1:1 Bismuth Molybdate

Line number	d (Å)	Relative intensity
1	3.1810	40
2	3.0440	5
3	2.8621	5
4	2.7968	22
5	2.6827	3
6	2.3411	3
7	2.2405	3
8	2.1685	3
9	2.0316	6
10	1.9852	10
11	1.9372	16
12	1.9103	4
13	1.8751	3
14	1.7989	2
15	1.6822	22
16	1.6353	12
17	1.5926	13
18	1.2627	10
19	1.2424	6
20	1.1389	5
21	1.1138	9

FIG. 1. Electron micrograph of an initial film prepared by the vacuum evaporation technique. It is clearly composed of very small particles.

results are consistent with those of Trifiro *et al.* (*15*), who in addition noticed traces of the 2:1 compound. Our samples as well as those of Dr. Batist show very similar characteristic lines. When heat treated under low pressure ($\sim 10^{-6}$ Torr) the material changed color from pale yellow to grey and concurrently intensities of some diffraction peaks were either depressed or disappeared completely. Oxygen depletion takes place in these conditions introducing defects and color centers for low depletions. For high depletions, essential modifications in the structure are expected.

b Thin Film Work

i. *Initial film.* Electron microscope observations revealed that the initial film formed by vacuum evaporation was fairly continuous and composed of very small particles. Films prepared in this manner are expected to be oxygen deficient. Electron diffraction patterns from such areas show diffuse halos and no diffraction lines, indicating that the film is amorphous. A typical electron micrograph and the corresponding diffraction pattern are shown in Figs. 1 and 2. Similar characteristics are present in all samples regardless of film thickness.

ii. *Films heated in air.* Thin films heated in air for 30 min at various temperatures crystallized and always underwent some changes in color—from greyish to light grey to light yellow. Initially, the films were annealed for only 30 min at different temperatures. As expected, the initial amorphous material crystallized and grain growth occurred along with the uptake of oxygen. Electron diffraction patterns from samples heated at 250 and 300°C were complex, containing two types of rings, continuous and spotted. As shown below, spotted rings correspond to a body centered tetragonal unit cell (scheelite structure) with parameters $a = b = 5.26 \pm 0.05$ Å, $c = 11.52 \pm 0.05$ Å and space group $I4_1/$

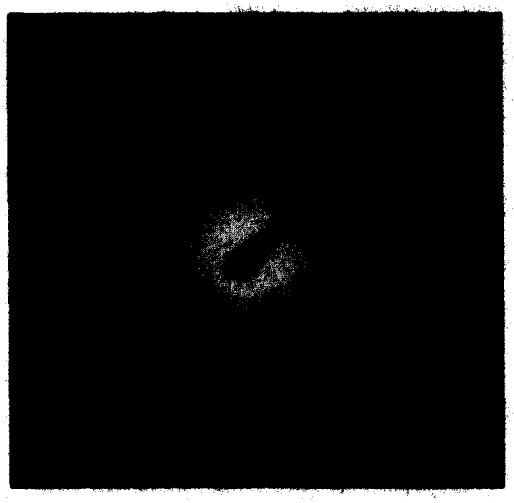

FIG. 2. Electron diffraction pattern of a film prepared by the vacuum evaporation technique. The diffuse halo indicates the presence of an amorphous phase.

$a(C_{4h}^6)$. Films heated at 350–400°C showed further grain growth and exhibited a peculiar phenomenon, viz, within the single grain a large number of small crystallites (domains) were generated (Fig. 3). This was also reflected in the diffraction pattern since besides the strong spots, secondary weak spots appeared (Fig. 4)—indicating the emergence of a superstructure in the matrix. Films heated at 500°C show such domain features more pronounced. At still higher temperatures, the films were found to rupture and eventually crumbled to a fine powder. In the latter case, when the rock salt crystal was immersed in water, fine powder spiraled all over and hence could no longer be taken over copper grids for further examination. Visual examination revealed that the structure of the small crystals (domains) formed during heat treatment in air is based on a pseudo fcc lattice. This suggests that a reordering of atomic species occurs in local regions during heat treatment as a result of the uptake of oxygen. Both nucleation and growth of the

FIG. 3. Electron micrograph showing small domains within the single grain after heating of the catalyst in air.

new domains were observed. These changes took place even during a heat treatment in air for as little as 30 min at 500°C.

To observe better the effect of annealing for different lengths of time, a lower temperature (250°C) was chosen since at higher temperatures the process was too fast. The initial amorphous films crystallized and exhibited complex diffraction pattern when heated at 250°C in air for short periods (30–60 min) but eventually gave rise after heating about 2 hr to the same peculiar phenomenon mentioned before, i.e., an inner substructure of domains developed within the grains (Fig. 5). The density of the domains and their size increased with temperature and time of calcination. As a result of heating and uptake of oxygen, the atomic species rearrange themselves in local regions, producing changes in stoichiometry. Therefore, both the temperature and time of calcination are crucial since diffusion of the atomic species is required for ordering to take place.

In order to determine the unit cell of the lattice corresponding to the crystals (domains) developed within the grains, several reciprocal lattice projections were recorded from different regions using the rotating-tilt stage in the transmission electron microscope. The diffraction patterns containing the secondary weak spots caused by the domains are presented in Fig. 6. All these could be consistently indexed by choosing a tetragonal unit cell with

$$|a|_t = |b|_t = a_0 \text{ and } |c|_t \simeq 2a_0 \quad c/a \sim 2,$$

where a_0 is the parameter of a pseudo fcc lattice. Looking more closely, it could be realized that the $|c|_t$ dimension is elongated such that the c/a ratio lies in the range of 2.16–2.22, and that the superstructure is derived from a pseudo fcc lattice with $a_0 \sim 5.32 \pm 0.05$ Å. In some regions it was possible to obtain diffraction patterns corresponding to the pseudo fcc lattice itself (Fig. 7). Erman and Galperin (*9*) noticed that in the 1:1 bismuth molybdate, Bi and Mo atoms form a pseudo fcc

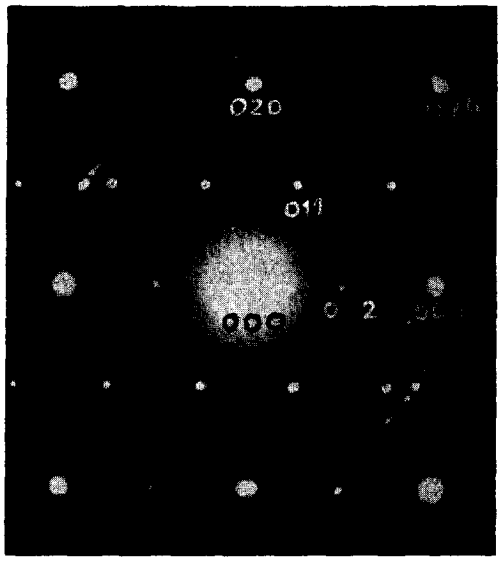

FIG. 4. Spot pattern showing additional secondary (smaller) spots due to the generation of a superstructure.

sublattice with parameter $a = 5.4$–5.6 Å. Though the lattice parameter of the pseudo fcc structure is in our case somewhat different, we believe that they represent the same lattice. The indices of the diffracted spots indicated in Fig. 6 have been assigned on the basis of the superlattice unit cell. From the systematic absence of spots for which $h + k + l$ is odd, it is concluded that the unit cell is body centered. The space group for this body centered tetragonal cell corresponding to the substructure of domains is $I\bar{4}m2$, the lattice parameter being approximately $|a|_t = |b|_t = 5.32 \pm 0.05$ Å, $|c|_t = 11.70 \pm 0.05$ Å with $c/a \simeq 2.2$. [The space group is among the four suggested by Erman *et al.* (*8*) for the 1:1 bismuth molybdate.] No correlation of the lattice parameter with thickness could be found. The variation was from sample to sample and place to place and could therefore be attributed to composition differences in local regions. The results discussed so far were found to occur for all film thicknesses except that of 50 Å. For the 50 Å thick film, only one kind of ring diffraction pattern was observed and no single crystal regions developed even after prolonged heating at

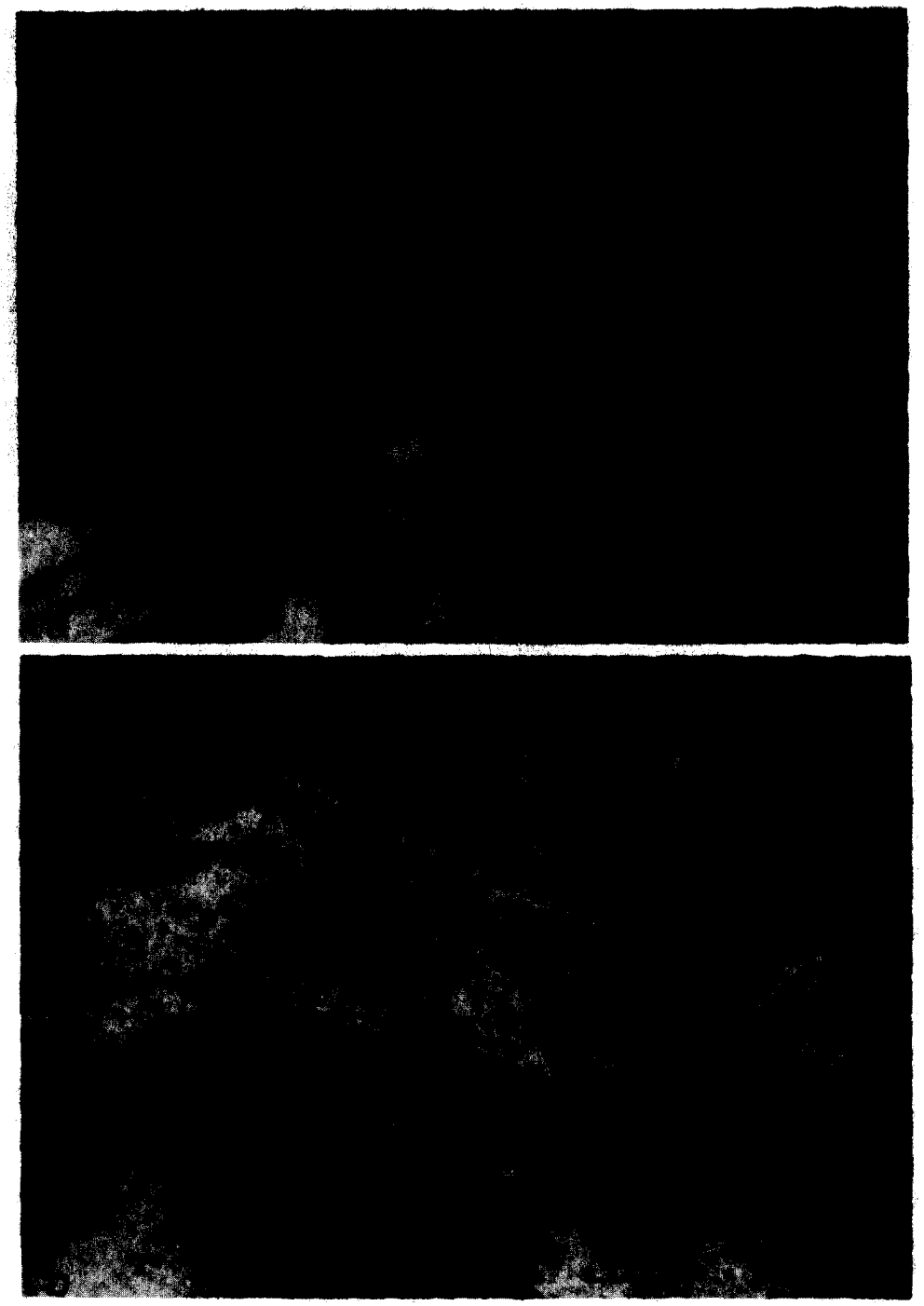

FIG. 5. Electron micrograph showing domain features after heating the initial amorphous film in air at 250°C for (a) 20 hr and (b) 28 hr.

250°C. Figure 8 shows the micrograph of such a film heated for 45 hr at 250°C in air. The diffraction lines which appear in this case were also present in the 400 and 700 Å films immediately after a short heat treatment (30–60 min) but the patterns in those

cases were somewhat more complex containing additional lines. However, in the 200 and 50 Å films, clear ring patterns were recorded which could be analyzed (Fig. 9) as characteristic of a tetragonal phase with the parameters $a = b = 5.26 \pm 0.5$ Å, $c = 11.52 \pm 0.05$ Å, and $c/a \simeq 2.19$. Slight variations in lattice parameters were noticed here too. From the systematic absences of lines, the unit cell was found to be body centered with the space group $I4_1/a(C_{4h}^6)$, corresponding to the tetragonal scheelite structure in which most of the tungstate and molybdates crystallize (*16*). In addition to these diffraction lines, rings corresponding to a face-centered cubic lattice with the parameter $a \simeq 5.4 \pm 0.5$ Å sometimes appeared. The *d*-values computed from the pattern shown in Fig. 9 are given in Table 2 along with the assigned indices.

iii. *Films annealed in vacuum.* Vacuum annealing of films gave rise to characteristics different from those reported above for air heating. In this case, besides the usual crystallization and grain growth further oxygen depletion is expected to occur. The presence of diffraction rings confirmed the crystallization of the original amorphous thin film. But the diffraction rings from samples annealed in vacuum at 230°C for 1 hr always gave rise to complex patterns and, therefore, posed difficulties in analysis. However, careful evaluation showed that most of the diffraction lines correspond to MoO_2, known to crystallize (*17*) in the monoclinic system with parameters $a = 5.608$ Å, $b = 4.843$ Å, $c = 5.517$ Å, $\beta = 119.75^0$ and space group $P2_1/c(C_{2h}^5)$. In addition, spotted rings, due to the traces of the scheelite structure, also appear in the background creating thereby a hazy picture.

Figure 10 depicts the electron micrograph of a 700 Å thick film annealed in vacuum and Fig. 11 is the corresponding electron diffraction pattern. In some regions metallic bismuth was also detected, in addition to MoO_2, and to the scheelite structure. The electron micrograph and diffraction from such areas are shown in Figs. 12 and 13. Films of 200 and 50 Å exhibited two kinds of characteristics. In some cases they exhibited more complex patterns containing broad rings, indicating thereby the presence of considerable disorder and strain in the films (Fig. 14). Even so, it was possible to verify the presence of MoO_2, of metallic bismuth and of the scheelite structure. A micrograph depicted in Fig. 15 shows the effect of vacuum annealing of the original amorphous film (50–200 Å). In some other cases, no diffraction patterns were observed and the corresponding electron micrograph showed particles smaller than those in Fig. 15.

It can be concluded that oxygen depletion (reduction) of the thin films of bismuth molybdate prepared under vacuum eventually yields MoO_2 and metallic bismuth. These observations are consistent with those cited by Schuit (*1*) but give direct visualization of the process as well.

We would like to mention that on repeating these experiments with samples obtained from Dr. Batist, the same results were obtained.

GENERAL DISCUSSION

1. Heating of the initially prepared amorphous films (corresponding to an oxygen deficient phase) in air leads to oxidation, recrystallization, and grain growth with the emergence of a scheelite structure. Further heating creates domains or superstructures within the already formed grains. The density of these domains increases with temperature and time of calcination. Growth of the domains also takes place. It is possible that the surface of the catalyst has patches with these structures. However, in regions where the catalyst looses oxygen for oxidation of unsaturated hydrocarbons, the structure might change to the scheelite type. The reduced patches trap oxygen from the gaseous atmosphere and undergo transformation back to the more oxidized structure. Therefore, during the catalytic process, a successive formation of scheelite-

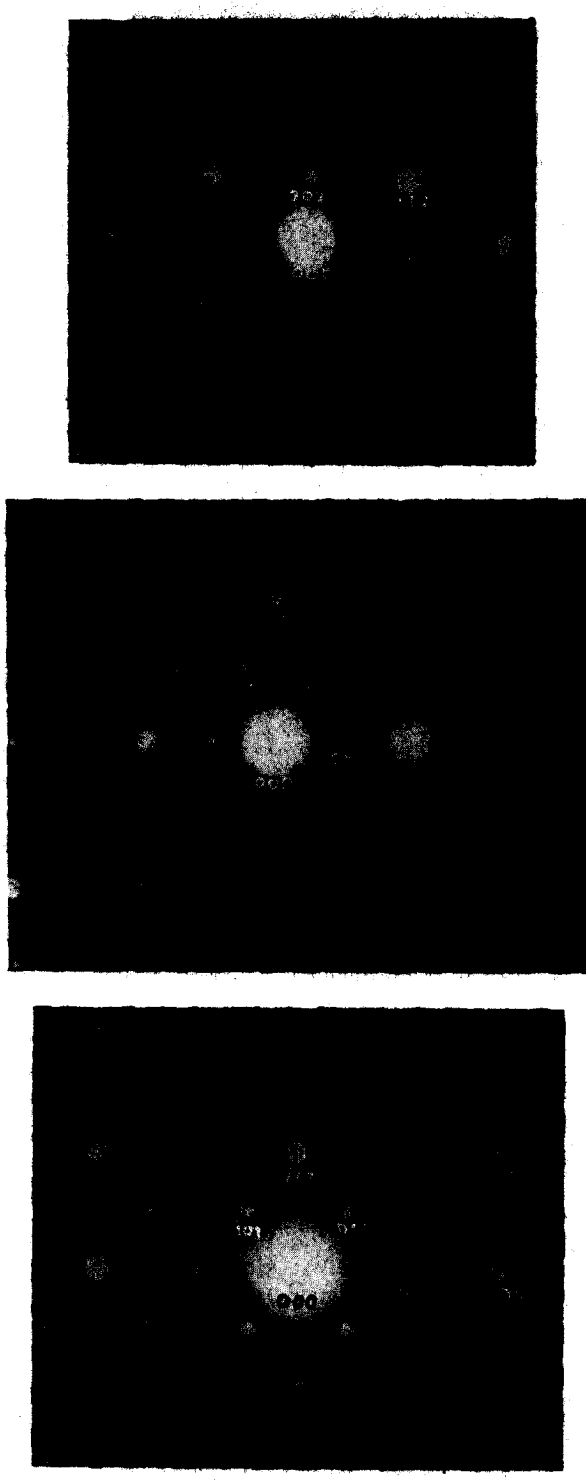

FIG. 6. Electron diffraction pattern from the domain substructure regions in orientations: (a) $(1\bar{1}0)$; (b) (100); (c) $(1\bar{1}1)$; (d) $(2\bar{2}1)$; (e) $(3\bar{1}1)$; (f) (120); (g) (011). The spots have been assigned indices on the basis of the superlattice unit cell.

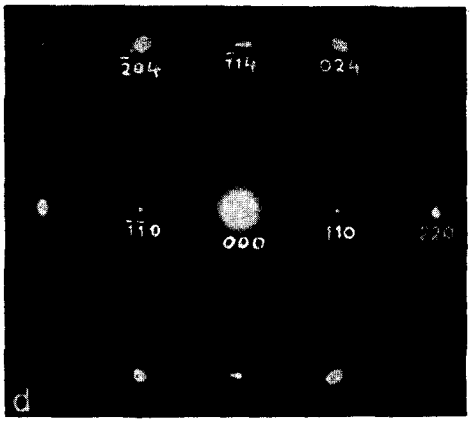

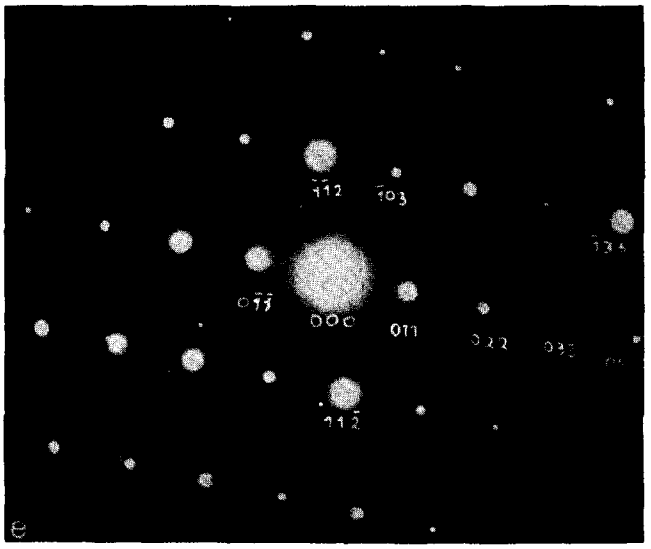

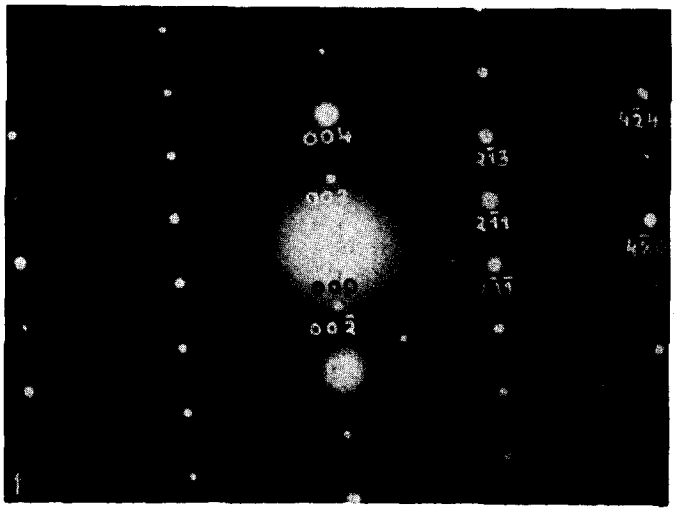

FIG. 6.—*Continued*

FIG. 6.—*Continued*

type structures (under reduction) and the more oxidized structure (under reoxidation) might occur near the surface. If there is no external oxygen supply, the consumption of lattice oxygen continues and finally the catalyst is reduced to a mixture containing the scheelite structure, MoO_2 and metallic bismuth.

2. Erman *et al.* (*8*) mentioned that the 1:1 bismuth molybdate might belong to the scheelite structure type. Obviously, this would have a tetrahedral configuration for the molybdenum ion. In the present investigation, a scheelite structure is indeed formed, which persists in films 50 Å thick even after prolonged heating in air. However, it changes to other structures in

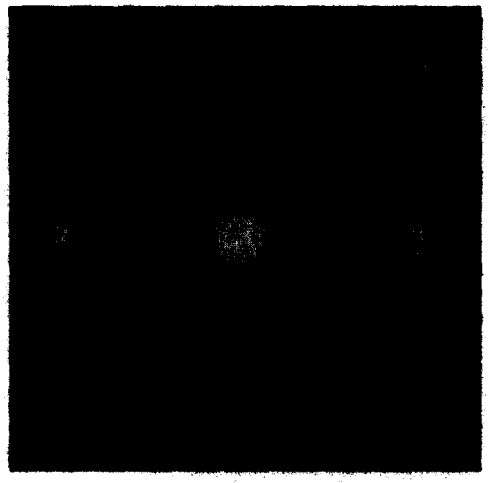

FIG. 7. Single crystal electron diffraction pattern of the pseudo fcc lattice in the (100) orientation.

TABLE 2

Interplanar Spacings Computed from Fig. 9 along with Their Assigned Indices

Line number	d (Å)	*hkl* (scheelite structure)	*hkl* (fcc lattice)
1	4.785	101	
2	3.122	112	111
3	2.883	004	
4	2.700	—	200
5	2.628	200	
6	2.394	202	
7	2.287	211, 114	
8	2.000	213	
9	1.948	204	
			220
10	1.852	220	
11	1.712	301	
12	1.640	215	311
13	1.592	312, 303	
14	1.561	224	222
15	1.441	231	
16	1.386	305	
17	1.358	323	400
18	1.311	400	

thicker films. It is interesting to note that an ideal scheelite structure having all the sites occupied corresponds to $Bi_2Mo_2O_8$ and contains less oxygen than the 1:1 bismuth molybdate $Bi_2Mo_2O_9$. The scheelite structure has also been found (*18*) to occur in bismuth molybdovates $Bi_{1-x/3}Mo_xV_{1-x}O_4$ for almost all values of x from 0.1 to values close to 1. It is also reported that vanadium atoms replace molybdenum statistically in this structure and random vacancies of bismuth ions occur to balance the difference of negative charges between the tetrahedral anions in the groups $(VO_4)^{3-}$ and $(MoO_4)^{2-}$. A similar structure was reported (*19*) for the bismuth iron molybdate system with atomic ratio Bi/Fe/Mo = 1:1:1. In view of these facts, we believe that in the scheelite structure either random vacancies of bismuth and molybdenum ions exist or/and changes in valency occur which assure electroneutrality and hence its stabilization. In order to accomodate more oxygen in this system, Mo ions change their valency and some rearrangements of Bi and/or Mo ions occur. This results in the nucleation and growth of the superstructure having a composition different from that of the scheelite structure. However, the 50 Å films are formed of a large number of small crystallites separated from each other. Therefore, even if the above requirement for accepting oxygen and forming a superstructure is met in some part of the crystallites, it will not show up in the diffraction patterns. This is presumably the reason that in the 50 Å films, the superstructure is not observed at 250°C even after prolonged heating in air.

Heating for a long time at the same partial pressure of oxygen, the scheelite structure might transform completely or

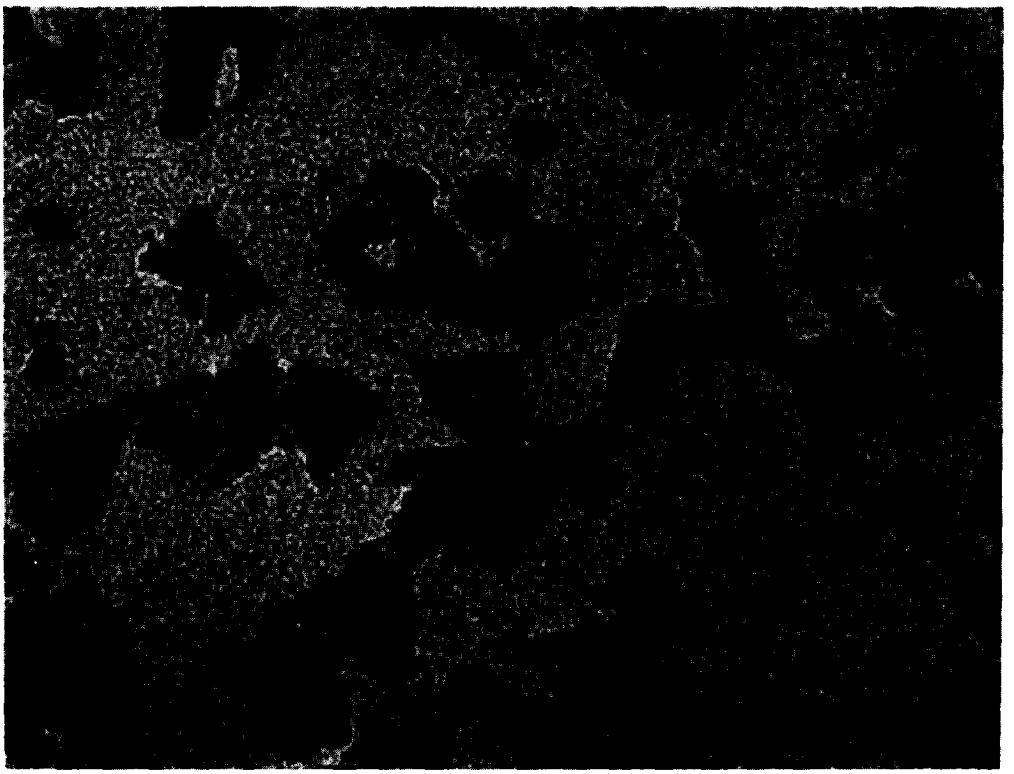

FIG. 8. Electron micrograph of a 50 Å thick film after calcination in air at 250°C for 45 hr. The particles are distributed.

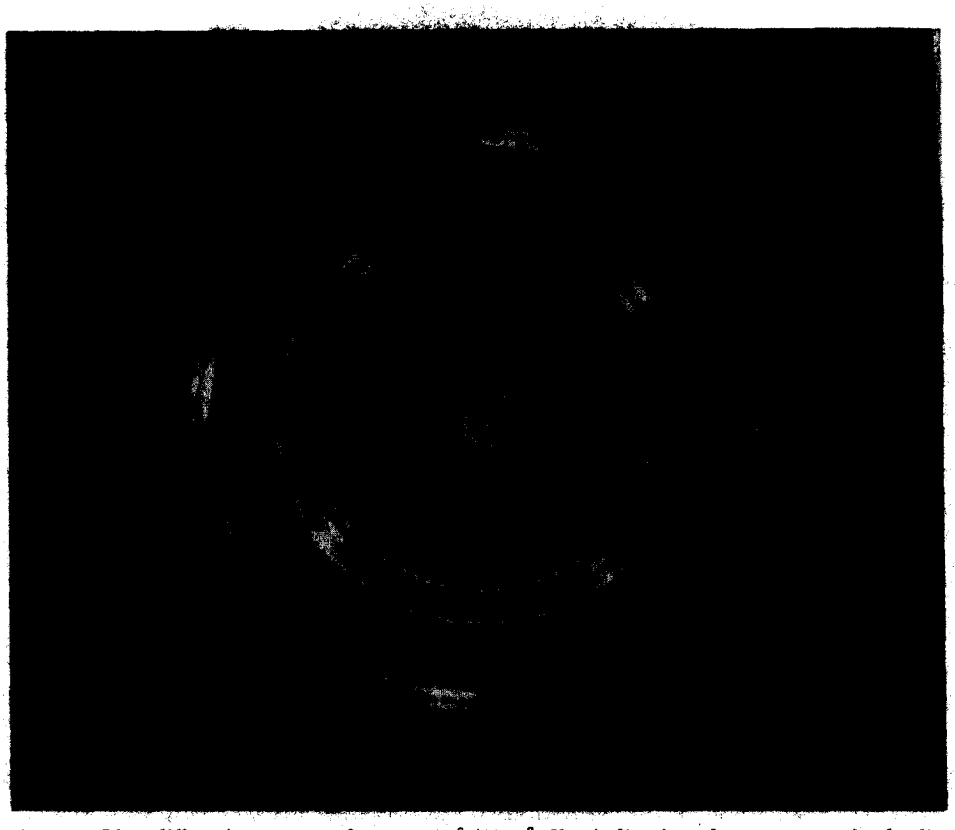

FIG. 9. Ring diffraction pattern from a 50 Å/200 Å film indicating the presence of scheelite-type tetragonal structure. The *d*-values and indices are given in Table 2. A few lines belonging to the pseudo fcc lattice are also detected and listed in Table 2.

only partially to the superstructure. In the first case a phase transformation occurs, while in the second a nonstoichiometric compound of the Ariya-type is generated. Ariya and Popov (*20*) hypothesized that in some conditions thermodynamically stable nonstoichiometric compounds (in particular oxides) are composed of small particles of one structure and valency dispersed in a matrix of another structure and valency. We suggest that such compounds are thermodynamically stable if the free energy change on "mixing" of the particles with the main matrix has a negative minimum for a given size of particles. The mixing involves the formation of an interface between the two phases. The corresponding free energy change is positive but small because the interfacial free energy is small, the structures being similar. The free energy change due to the formation of a double layer near the interfaces is negative, while the intraparticular repulsive forces caused by charged interfaces generate also a positive contribution to the free energy. In addition, the entropic effect caused by the random distribution of particles has a negative contribution to the free energy. If the interfacial free energy is small enough, the free energy of formation of the double layer as well as the entropy contribution can overcome the increase caused by the creation of interfacial areas and the dispersed system will be stable from a thermodynamic point of view for a given size of the particles. A theoretical approach along these lines was developed previously by Ruckenstein and Chi (*21*) in a related problem concerning the stability of microemulsions. A choice between

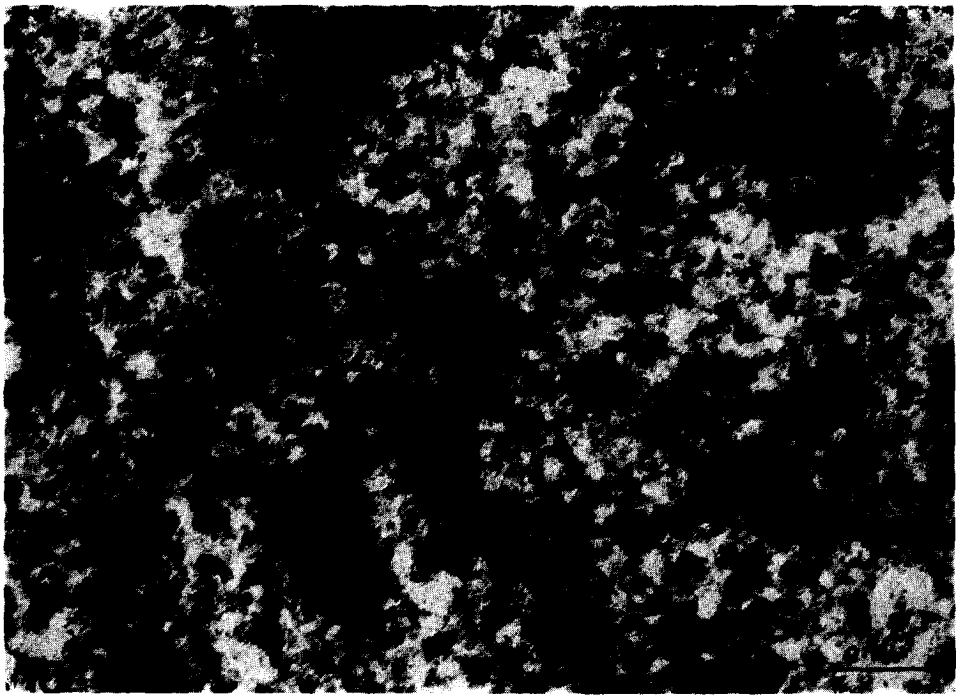

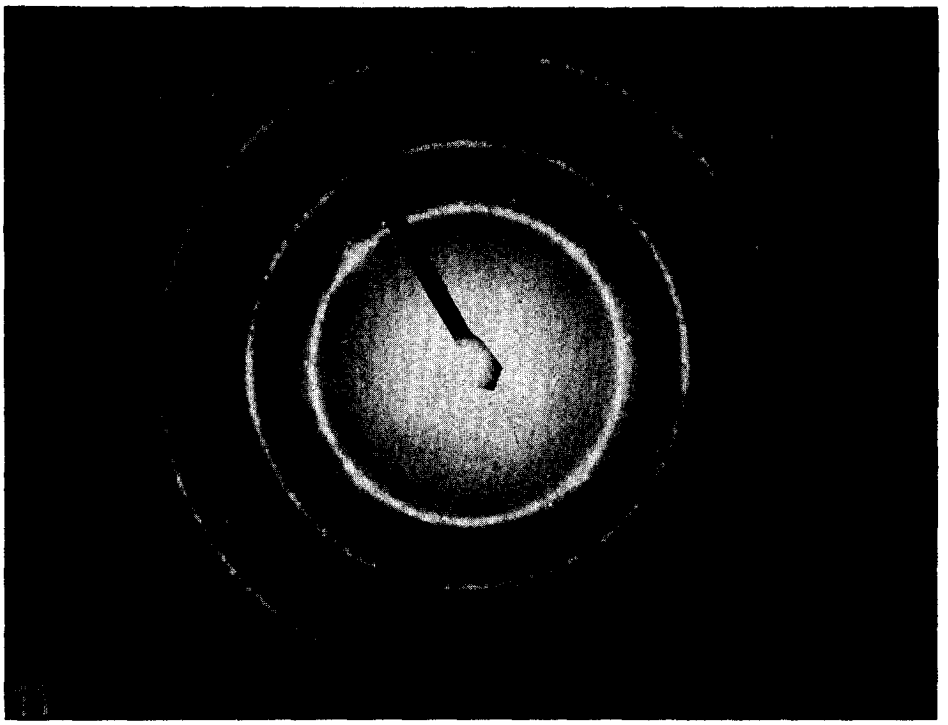

FIGS. 10 and 11. Electron micrograph and diffraction pattern of a 700 Å thick film annealed in vacuum, indicating the presence of MoO_2 and scheelite structure.

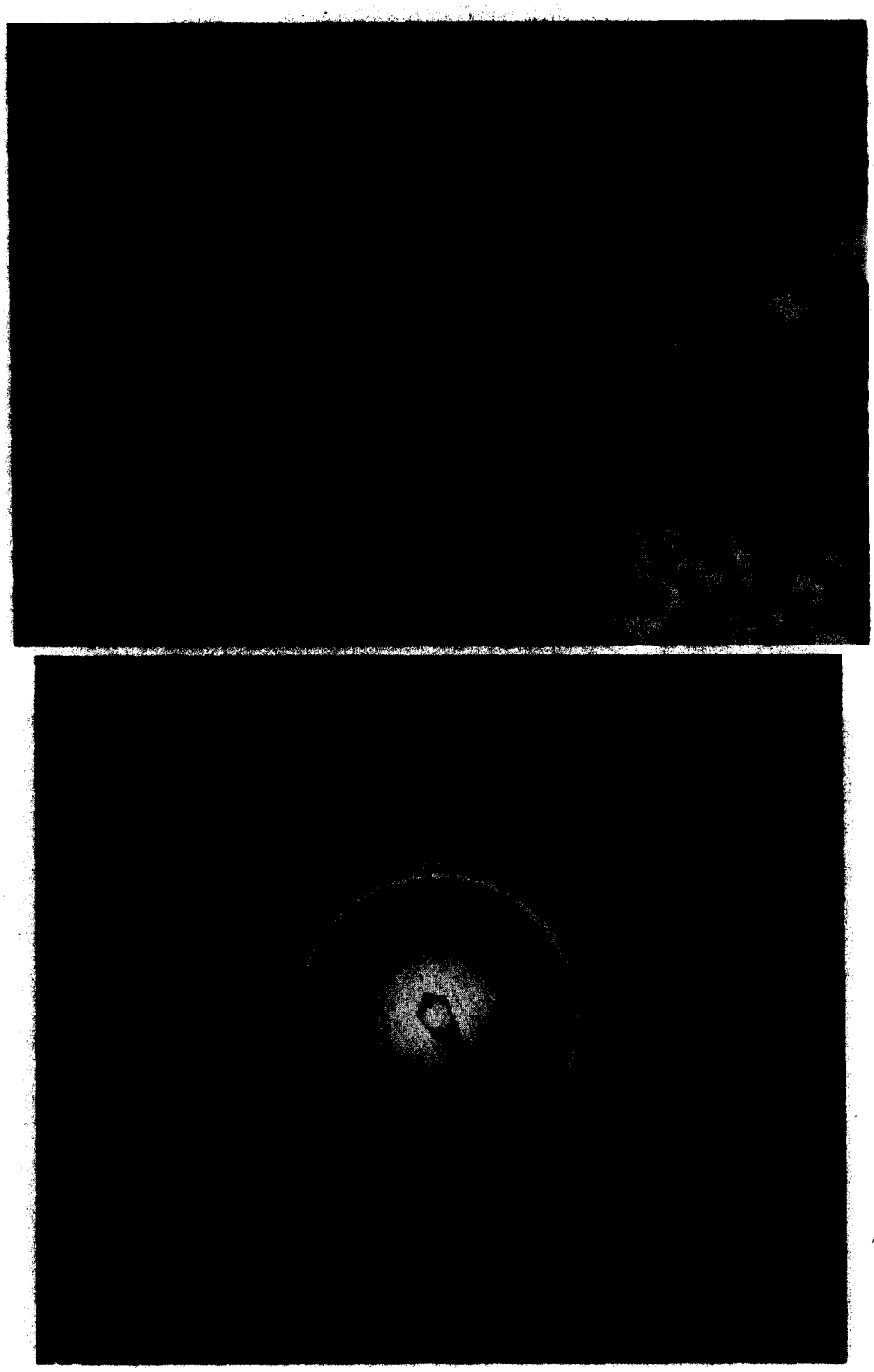

FIGS. 12 and 13. Electron micrograph and diffraction pattern of a 400 Å thick film annealed in vacuum, indicating the presence of MoO_2, scheelite structure and metallic bismuth.

the two possibilities mentioned at the beginning of this paragraph cannot be made on the basis of the present experimental information.

3. Batist *et al.* (*4*) tried to correlate the bulk crystal structure of bismuth molybdate with their catalytic properties. In their opinion, the catalytic activity for selective oxidation of olefins is connected with the presence of corner-sharing Mo–O octahedra, while the catalytic activity is largely absent in compounds containing edge-shared octahedra. They believe that in the 1:1 compound the Mo ion has an octahedral coordination which allows a high catalytic activity. Also, they suggest that interlinking of Mo–O octahedra by edge sharing is responsible for the low activity of the 2:3 molybdate. However, detailed study (*6*, *7*) has shown that in the 2:3 compound, the molybdenum ion is surrounded by a distorted tetrahedron. Infrared and ultraviolet investigations (*10*) have revealed the presence of both the tetrahedral and octahedral oxomolybdenum species on the surface of the 2:1 and 1:1 active bismuth molybdates. At temperatures up to 320°C, the 2:1 compound undoubtedly exhibits (*6*) distorted Mo–O octahedra with corner sharing but it transforms (*22*, *23*) at 550–640°C to the Blasse phase, in which a tetrahedral configuration occurs for molybdenum ions. Catalytic processes are, however, carried out at intermediate temperatures (350–500°C) at which the 2:1 compound undergoes a phase transformation (*22–23*) and therefore the resulting structure may contain either an altogether different coordination or a mixed one having both the

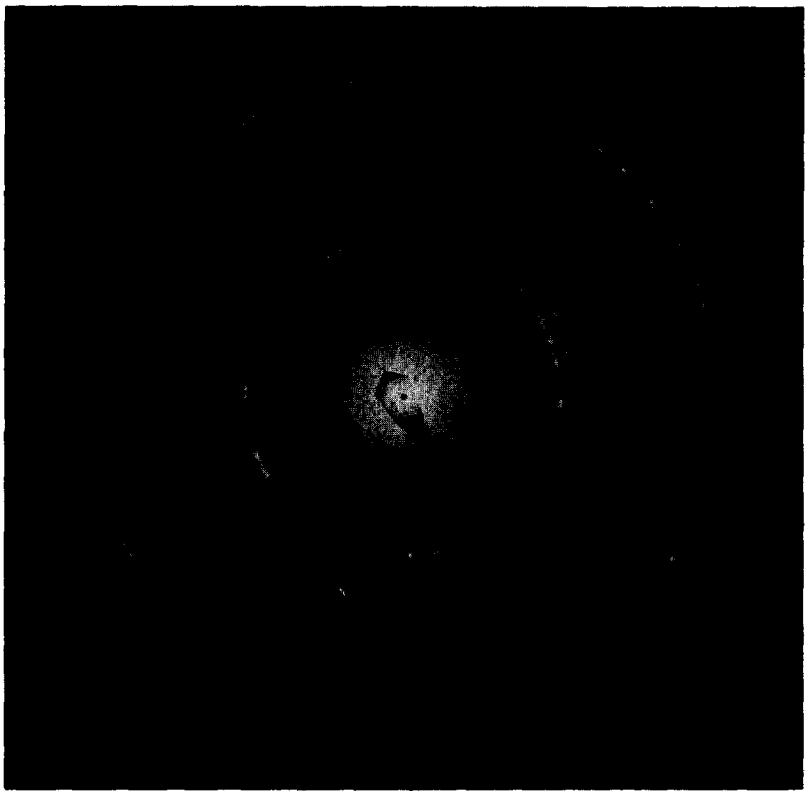

FIG. 14. Complex diffraction pattern obtained for 200 and 50 Å thick films when annealed in vacuum—show up broad rings. The presence of scheelite structure, MoO_2 and metallic bismuth is noted.

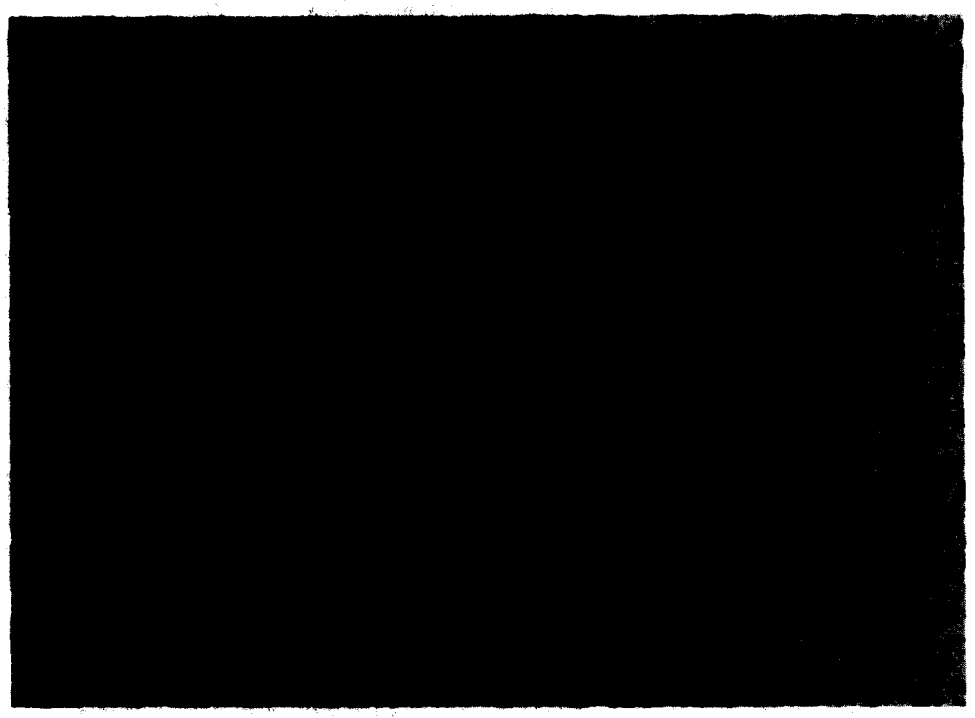

FIG. 15. Electron micrograph from the region corresponding to Fig. 14.

tetrahedral and octahedral coordination for the molybdenum ion.

In thin films of the 1:1 compound two structures have been identified in the present paper during heating in air: a scheelite structure in which the Mo ions have a tetrahedral coordination of oxygen, and the superstructure in which the coordination is modified from the tetrahedral without being octahedral.

CONCLUSIONS

1. Thin films of 1:1 bismuth molybdate 50–700 Å thick prepared by vacuum evaporation technique are amorphous and oxygen deficient. Vacuum annealing of these films resulted in further depletion of oxygen along with crystallization. This depletion eventually yields MoO_2, and metallic bismuth with traces of the scheelite structure of bismuth molybdate.

2. Air annealing of the originally prepared amorphous films leads both to oxidation and recrystallization. A scheelite phase structure with a tetragonal cell having $a = b = 5.26 \pm 0.05$ Å and $c = 11.52 \pm 0.05$ Å is formed in all the films at the beginning and survives in the 50 Å thick films even after prolonged heating. However, in films 200–700 Å thick, further heating in air showed nucleation and growth of new crystallites within the original grains, indicating some rearrangement of the atomic species in local regions. The new crystallites have a body-centered tetragonal lattice with parameters $a = b = 5.32 \pm 0.05$ Å, $c = 11.70 \pm 0.05$ Å, $c/a \sim 2.2$. While the scheelite structure has a tetrahedral configuration for Mo ions, the superstructure is modified from the tetrahedral without being octahedral.

3. It is expected that these structures occur near the catalyst surface during the catalytic oxidation. In patches of the surface that are depleted of oxygen, a scheelite structure might form which would change to the superstructure with the help of the gaseous oxygen.

4. The occurrence of the new crystallites within the grains generates nonstoichiometric compounds. The hypothesis formulated by Ariya and Popov (*20*) that some nonstoichiometric compounds contain within the initial compound a dispersion of small particles with a different composition is justified on the basis of a thermodynamic argument.

ACKNOWLEDGMENT

We are indebted to Dr. Ph. A. Batist for providing us with samples for comparison. This work was supported by the National Science Foundation.

REFERENCES

1. Schuit, G. C. A., *J. Less Common Metals* **36**, 329 (1974).
2. Van der Wiele, K., and Van den Berg, P. J., *J. Catal.* **39**, 437 (1975).
3. Hucknall, D. J., "Selective Oxidation of Hydrocarbons," p. 33. Academic Press, New York, 1974.
4. Batist, P. A., Der Kinderen, A. H. W., Leeuwenburgh, Y., Metz, F. A. M. G., and Schuit, G. C. A., *J. Catal.* **12**, 45 (1968).
5. Boutry, P., Montarnal, R., and Wkzysrez, J., *J. Catal.* **13**, 75 (1969).
6. Van Elzen, A. F., and Rieck, G. D., *Acta Crystallogr.* **B29**, 2433 and 2436 (1973).
7. Zemann, J., *Heidelb. Beitr. Miner. Petrog.* **5**, 139; (1956); *Acta Crystallogr.* **7**, 630 (1954) (Abstr.).
8. Erman, L. Y., Galperin, E. L., Kolchin, I. K., Dobrzhanskii, G. F., and Khernyshev, K. S., *Russ. J. Inorg. Chem.* **9**, 1174 (1964).
9. Erman, L. Y., and Galperin, E. L., *Russ. J. Inorg. Chem.* **11**, 122 (1966); **13**, 441 (1970).
10. Mitchell, P. C. H., and Trifiro, F., *J. Chem. Soc. A* **18**, 3183 (1970).
11. Fattore, V., Fuhrman, Z. A., Manara, G., and Notari, B. J., *J. Catal.* **37**, 215 (1975).
12. Chopra, K. L., "Thin Film Phenomena," p. 189. McGraw-Hill, New York, 1969.
13. Andrews, K. W., Dyson, D. J., and Keown, S. R., "Interpreparation of Electron Diffraction Patterns," p. 15. Plenum, New York, 1971.
14. Batist, P. A., Bouwens, J. F. H., and Schuit, G. C. A., *J. Catal.* **25**, 1 (1972).
15. Trifiro, F., Hoser, H., and Scark, R. D., *J. Catal.* **25**, 12 (1972).
16. Sillen, L. G., and Nylander, A. L., *Ark. Kemi, Min. Geol.* **17A**, 1 (1943).
17. Magneli, A., and Anderson, G., *Acta Chem. Scand.* **9**, 1378 (1955).
18. Cesari, M., Pergo, G., Zazzetta, A., Manana, G., and Notari, B., *J. Inorg. Nucl. Chem.* **33**, 3595 (1971).
19. Notermann, T., Keulks, G. W., Skliarov, A., Maximov, Y., Margolis, L. Y., and Krylov, O. V., *J. Catal.* **39**, 286 (1975).
20. Ariya, S. M., and Popov, Y. G., *Russ. J. Gen. Chem.* **32**, 2077 (1962).
21. Ruckenstein, E., and Chi, J. C., *J. Chem. Soc., Faraday Trans. II* **71**, 1690 (1975).
22. Erman, L. Y., and Galperin, E. L., *Russ. J. Inorg. Chem.* **13**, 487 (1968).
23. Erman, L. Y., Galperin, E. L., and Sobolev, B. P., *Russ. J. Inorg. Chem.* **16**, 258 (1971).